BmSPN2, a Serpin Secreted by the Filarial Nematode *Brugia malayi*, Does Not Inhibit Human Neutrophil Proteinases but Plays a Noninhibitory Role†

Peter Stanley and Penelope E. Stein*

Division of Structural Medicine, Department of Haematology, Cambridge Institute for Medical Research, Wellcome Trust/MRC Building, Hills Road, Cambridge, CB2 2XY, United Kingdom

Received November 12, 2002; Revised Manuscript Received March 21, 2003

ABSTRACT: The filarial nematode, *Brugia malayi*, is a causative agent of lymphatic filariasis. *Bm-spn-2*, one of two serpin genes identified in *B. malayi*, is expressed only in humans where the encoded protein, BmSPN2, is secreted by blood-dwelling microfilariae. Previous work reported that BmSPN2 could inhibit the activities of elastase and cathepsin G from human neutrophils, despite an atypical amino acid sequence. This did not fit with accepted theories as to the sequence requirements of serpins for proteinase inhibition. We have cloned and expressed *Bm-spn-2* in *Escherichia coli* and characterized the structural and functional properties of recombinant BmSPN2. Sequence alignment, circular dichroism spectroscopy, and susceptibility to cleavage by proteinases all suggest that BmSPN2 shares the tertiary structure typical of the serpin family including an accessible reactive center loop. However, we have found that BmSPN2 has no effect on the activity of neutrophil elastase or cathepsin G and does not form SDS-stable complexes with these proteinases. We provide evidence that BmSPN2 cannot undergo the characteristic stressed to relaxed transition required for proteinase inhibition by serpins. We conclude that BmSPN2 is not an atypical inhibitor but is a new noninhibitory serpin, in keeping with its sequence.

The serpins (*1*, *2*) are a superfamily of homologous proteins that mostly act as serine proteinase inhibitors. Serpins in human plasma control the major proteolytic pathways including blood coagulation, fibrinolysis, complement activation, and inflammation. Unlike typical proteinase inhibitors, the serpins have a highly mobile reactive center loop. The reactive site acts as a peptide bait for the target proteinase, which cleaves the serpin between residues at the P1 and P1′ positions. Cleavage is accompanied by an extraordinary topological transformation in which the cleaved reactive loop of the serpin drags the tightly attached proteinase along the length of the molecule, causing deformation of the proteinase that results in irreversible inhibition (*3*). The cleaved loop becomes inserted in the center of the serpin molecule as a new strand in a large β-sheet (sheet A), and the serpin is converted from its native stressed (S) conformation to a more stable relaxed (R) form (*4*).

A few serpins show no inhibitory activity, and the conserved framework of the molecule has apparently been adapted for new functions. Examples of noninhibitory serpins include angiotensinogen (*5*), which acts as the donor of a vasoactive peptide, and heat shock protein 47 (*6*), which plays a role in collagen folding. Almost all the noninhibitory serpins appear to be fixed in a native conformation resembling the uncleaved active (S) conformation of inhibitory serpins. With a few exceptions (*7*), the S to R transition is considered to be a predictive marker for serpins with inhibitory potential.

Two serpins have been identified in the filarial nematode *Brugia malayi*, a causative agent of lymphatic filariasis. Filarial nematodes are transmitted to their human hosts by mosquitoes. They migrate to the lymphatic vessels where sexually reproducing adult worms release millions of microfilariae into the bloodstream. Adult worms may live for more than 7 years in their host and microfilariae may survive in the blood for at least a year, but the mechanisms by which the parasite evades the human immune response are poorly understood.

The two serpin genes in *B. malayi*,[1] *Bm-spn-1*, and *Bm-spn-2* (*8*, *9*) are not closely related phylogenetically. *Bm-spn-1* is expressed during most stages of the parasite's life cycle, but *Bm-spn-2* is expressed only in the microfilarial stage, where it represents greater than 2% of the mRNA (*9*). The gene products, BmSPN1 and BmSPN2, share sequence identity of only 28%. BmSPN2 contains 428 amino acids including a putative signal peptide (amino acids 1−20) and is secreted into the bloodstream. A previous study (*9*) found that recombinant BmSPN2 appeared to inhibit the activities of elastase and cathepsin G from human neutrophils although it has an atypical reactive center sequence for an inhibitory serpin with a hinge sequence from P15-P10 of GINNEN (Figure 1). To resolve this ambiguity, we have carried out further studies of the protein. BmSPN2 was recloned, and a

† This work was funded by the Wellcome Trust (Grant 054518/Z/98/Z).

* To whom correspondence should be addressed. Tel: 44 1223 762660. Fax: 44 1223 336827. E-mail: pes1000@cam.ac.uk.

[1] Abbreviations: *B. malayi*, *Brugia malayi*; *E. coli*, *Escherichia coli*; *S. aureus*, *Staphylococcus aureus*; PMSF, phenyl methane sulfonyl fluoride; AEBSF, aminoethyl benzenesulfonyl fluoride; IPTG, isopropyl-β-D-thiogalactopyranoside; SDS−PAGE, sodium dodecyl sulfate polyacrylamide gel electrophoresis; CD, circular dichroism; TUG, transverse urea gel; BSA, bovine serum albumin; tPA, tissue plasminogen activator; HNE, human neutrophil elastase; CatG, human neutrophil cathepsin G.

10.1021/bi0271650 CCC: $25.00
Published on Web 05/02/2003

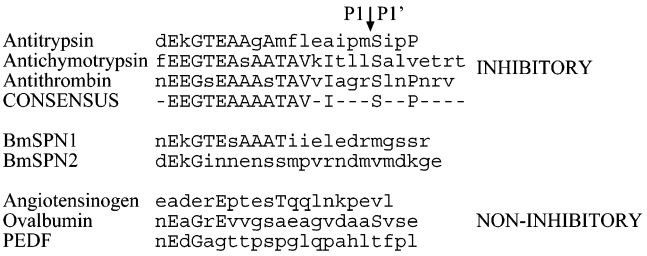

FIGURE 1: Primary structure of the reactive center loops of BmSPN1, BmSPN2, and other serpins. Comparison of the amino acid sequences from P18-P4′ of three inhibitory serpins (human antitrypsin (*27*), antichymotrypsin (*28*), and antithrombin (*29*)) and three noninhibitory serpins (human angiotensinogen (*30*), chicken ovalbumin (*31*), and human pigment epithelium-derived factor (*32*)) with the reactive center regions of BmSPN1 (*8*) and BmSPN2 (*9*). The position of the reactive site is arrowed.

second natural variant was identified. Both variants were expressed in *Escherichia coli* and found to behave identically. We provide evidence that BmSPN2 does not function as a proteinase inhibitor although it shares many structural features common to other serpins.

EXPERIMENTAL PROCEDURES

Materials. Human neutrophil elastase, cathepsin G, α1-antitrypsin, and α1-antichymotrypsin were from Athens Research and Technology (Athens, GA); human thrombin, Factor Xa, plasmin, T4 DNA ligase, and AEBSF (Pefabloc) were from Roche; chicken egg albumin, tPA, and Protease Inhibitor Cocktail Set III were from Calbiochem; restriction enzymes were from New England Biolabs (Hitchin, UK); Factor Xa was from Novagen; Bradford assay reagent was from Pierce; polyacrylamide gel protein markers were from Bio-Rad; ampicillin, chloramphenicol, tetracycline, and isopropyl-1-β-D-thiogalactopyranoside (IPTG) were from Melford Labs. Ltd. (Ipswich, UK); recombinant human antichymotrypsin and His-tagged antitrypsin were gifts from Drs. D. Crowther and A. Zhou, respectively; antibody to BmSPN2 was a gift from Prof. R. Maizels (University of Edinburgh); and oligonucleotides were purchased from the Protein and Nucleic Acid Facility, Department of Biochemistry, University of Cambridge. All other reagents were purchased from Sigma.

Vector Construction of Recombinant BmSPN2. A cDNA fragment encoding BmSPN2 was isolated from a *B. malayi* microfilarial cDNA library (*10*) by PCR amplification performed with primers 5′-CGCGCATATGAACAGTACTTTAAACCA-3′ (nt 87−103) and 5′-GCATATGTTATTCAACATCATATTT-3′ (nt 1403−1386). The resulting 1.2 kbp product was ligated into pGEM-T vector (Promega), transformed into *E. coli* JM109 (New England Biolabs), and verified by DNA sequencing of the entire *Bm-spn2* gene. A 1.3 kbp *Nde* I fragment was subcloned into pET16b (Novagen) to allow expression of BmSPN2 with a cleavable N-terminal $His_{(10)}$-tag.

As compared to the original sequence (ref *9*, Table 1), our construct had two point mutations within the coding region and one 4 bp insertion downstream of the coding region, which encoded two amino acid substitutions, P221A and V225I. Mutagenesis of our expression construct (pET-BmSPN2AI) to give the original sequence (pET-BmSPN2PV) was accomplished using the complementary oligonucleotides 5′-CCGTTCTATTCACCACGGCTACGCGTAACTGATATGCC-3′ (nt 675−712) and 5′-GGCATATCAGTTACGCGTAGCCGTGGTGAATAGAACGG-3′ and the QuikChange Site-directed Mutagenesis protocol (Stratagene). Since both sequences probably reflected natural proteins, both variants were expressed, purified, and compared in all experiments.

Table 1: Comparison of DNA Sequences and Predicted Amino Acid Sequences of the Two Natural Variants of BmSPN2[a]

	BmSPN2PV		BmSPN2AI	
nucleotide	DNA sequence	amino acid	DNA sequence	amino acid
687	CCA	Pro (221)	GCA	Ala
699	GTA	Val (225)	ATA	Ile
1346	TA		TGATAA	

[a] Amino acids are given in single letter code. Numbering corresponds to the derived sequence from the *Bm-spn-2* cDNA where nucleotide 27 initiates the codon for the fMet residue (*1*) of the precursor BmSPN2 polypeptide (*9*).

Expression and Purification of Recombinant BmSPN2. Expression and purification of recombinant BmSPN2 in *E. coli* were carried out as described previously (*9*). Competent BL2l (DE3) *recA* (pLysS) cells were transformed with the BmSPN2 cDNA-containing pET16b plasmids and selected on Luria Broth plates containing ampicillin (Ap, 50 μg/mL), chloramphenicol (Cm, 25 μg/mL), and tetracycline (Tc, 25 μg/mL). Single colonies were used to inoculate LB containing 2% glucose, Ap, Cm, and Tc incubated at 37 °C to an OD_{600} 0.8, and expression was induced with the addition of IPTG. The cells were incubated for an additional 4 h at 25 °C, collected by centrifugation, and resuspended in 20 mM Tris, 500 mM NaCl, 5 mM imidazole (pH 8.0). The cells were sonicated on ice, and the soluble fraction was collected after spinning for 20 min at 16 000*g*. Cleared lysate was loaded onto 2.5 mL His-Bind resin (Novagen) equilibrated with 20 mM Tris, 500 mM NaCl, 5 mM imidazole, pH 8.0. The column was washed with 20 mM Tris, 500 mM NaCl, 5 mM imidazole, pH 8.0, followed by 20 mM Tris, 500 mM NaCl, 60 mM imidazole, pH 8.0 and finally 20 mM Tris, 150 mM NaCl, pH 8.0 before eluting BmSPN2 with 20 mM Tris, 150 mM NaCl, 50 mM EDTA, pH 8.0. After nickel affinity chromatography, BmSPN2 was further purified by gel filtration chromatography on a HiLoad 16/60 Superdex 200 column (Amersham Pharmacia Biotech) equilibrated with 20 mM Tris, 150 mM NaCl, 5 mM EDTA, pH 8.0. The protein was concentrated in a 30k cutoff spin concentrator (Vivascience) and filtered through a 0.2 μm spin filter (Amicon). Protein quantitation was performed using the micro-Bradford assay with bovine serum albumin (Fraction V; BDH) as standard.

The N-terminal $(His)_{10}$-tag on BmSPN2 was removed by cleavage with Factor Xa. After the reaction, Factor Xa was removed by capture on Xarrest Agarose, and uncleaved BmSPN2 was removed by capture on a His-Bind resin Quick 300 cartridge (Novagen).

Design of Experiments. All experiments were carried out using four different protein preparations in parallel: BmSPN2PV with and without the His-tag and BmSPN2AI with and without the His-tag.

Proteinase Inhibition Studies. The ability of BmSPN2 to inhibit human neutrophil elastase (HNE) and cathepsin G

(CatG) was assayed in solution using chromogenic substrates. 0.8 μM proteinase and 0−35 μM BmSPN2 were incubated at room temperature for 10 min in 145 μL of 20 mM Tris, 150 mM NaCl, pH 8.0. Reactions of proteinase with BSA were assayed under identical conditions. Equivalent reactions were performed between BmSPN2 and HNE or CatG in which the total protein concentration was kept constant at 35 μM by addition of BSA and between α1-antitrypsin with HNE and α1-antichymotrypsin with CatG as controls. Residual proteinase activities were determined in duplicate aliquots by addition of 0.9 mL of 1 mM *N*-methoxysuccinyl-Ala-Ala-Pro-Val-*p*-nitroanilide in 50 mM Tris-Cl, 300 mM NaCl, 0.1% PEG8000, pH 7.5 for HNE or 0.9 mL of 1 mM *N*-succinyl-Ala-Ala-Pro-Phe-*p*-nitroanilide in 50 mM Tris-Cl, 600 mM NaCl, 0.1% PEG8000, pH 7.5 for CatG. Increases in absorbance at 405 nm were monitored on a Shimadzu UV-1601 spectrophotometer at 25 °C. The rates of substrate hydrolysis were linear to a maximal 205 mAbs/min/μg for HNE and 19 mAbs/min/μg for CatG. Reactions with BmSPN2 were repeated under identical conditions in the presence of 1 mg/mL heparin.

The ability of BmSPN2 to form SDS-stable complexes with HNE and CatG was studied in reaction mixtures containing a 4.5:1 molar ratio of serpin to proteinase. 50 μg of BmSPN2 was incubated with 5 μg of proteinase for 5 and 20 min at room temperature in 60 μL of 20 mM Tris, 150 mM NaCl, pH 8.0. Reactions were stopped by the addition of SDS−PAGE sample buffer and snap freezing in liquid nitrogen. Samples were run on duplicate 10% polyacrylamide gels. One gel was stained with Coomassie brilliant blue, and the other was used for transfer to PVDF membrane for Western blot analysis with a Ni-NTA HRP conjugate. Reaction mixtures of HNE with α1-antitrypsin and CatG with α1-antichymotrypsin were assayed under identical conditions as controls for Coomassie blue stained gels, and a reaction mixture of HNE with a recombinant His-tagged α1-antitrypsin was the control for immunoblotted gels.

Reactions between BmSPN2 and chymotrypsin, Factor Xa, pancreatic elastase, papain, plasmin, subtilisin, thermolysin, thrombin, tPA, trypsin, urokinase, and V8 protease were analyzed by SDS−PAGE to check for the formation of SDS-stable complexes.

Preparation of Reactive Center Loop-Cleaved BmSPN2. BmSPN2 was treated with HNE at a 20:1 molar ratio for 20 min at 25 °C in 20 mM Tris-Cl, 150 mM NaCl, pH 8.0. Cleavage was confirmed by SDS−PAGE and N-terminal sequencing of the products. Cleaved BmSPN2 was separated from HNE and other products by gel filtration, and cleaved His-BmSPN2 was purified by extraction on a His-Bind resin Quick 900 cartridge (Novagen). Antitrypsin was cleaved at the reactive center loop by incubating with *S. aureus* V8 proteinase (*11*) as a control.

Heat Stability Assays. Thermal stability studies were carried out on BmSPN2, HNE-cleaved BmSPN2, human α1-antitrypsin, and *S. aureus* V8 proteinase-cleaved α1-antitrypsin. Aliquots of native and cleaved protein were incubated at 0.1 mg/mL between 30 and 90 °C for 2 h as previously described (*5*), and residual protein was quantified by densitometry of Coomassie blue stained gels using Quantity One (Bio-Rad).

Circular Dichroism. CD spectra were recorded between 195 and 250 nm on a Jasco J-810 spectropolarimeter with 0.15−0.25 mg/mL protein in 10 mM sodium phosphate buffer (pH 7.9). Each spectrum represents the average of five scans. Two such spectra were averaged, and the data was smoothed. Thermal denaturation was followed by monitoring the CD signal at 222 nm as a function of temperature. Melting points (T_m) were calculated using an expression for a two state transition as described previously (*6*, *12*). Data were smoothed and averaged over at least two experiments.

Polyacrylamide Gel Electrophoresis. The discontinuous system of Schagger and von Jagow (*13*) was used for SDS−polyacrylamide gel electrophoresis. For nondenaturing polyacrylamide gel electrophoresis, two discontinuous buffer systems were used. An alkaline gel system (*14*) was used for antitrypsin and an acid buffer system for BmSPN2 (85 mM acetic acid, pH 6.5 in the stacking gel, 350 mM acetic acid, pH 4.3 in the separating gel, and 0.1 M β-alanine pH 4.2 as the running buffer). Transverse urea gradient gel electrophoresis was carried out on BmSPN2, HNE-cleaved BmSPN2, human α1-antitrypsin, and *S. aureus* V8 proteinase-cleaved α1-antitrypsin using both acid and alkaline buffer systems (*15*). 10% (w/v) polyacrylamide gels were cast with a linear gradient from 0 to 8 M urea.

Sequence Analysis. All DNA sequencing was performed on an Applied Biosystems Prism 310 Genetic Analyzer by the ABI PRISM Big Dye Terminator cycle sequencing method (Perkin-Elmer). N-terminal amino acid sequence determination was performed using an Applied Biosystems model 477 sequencer.

Immunoblotting. Proteins were transferred to Immobilin-P membrane and incubated with either mouse antisera to recombinant BmSPN2 (*9*) and then with peroxidase-conjugated rabbit antimouse IgG (Sigma) or with Ni-NTA HRP conjugate (Qiagen). Bound peroxidase was detected by chemiluminescence on the addition of the luminol-based ECL substrate (Amersham Pharmacia Biotech).

RESULTS

Expression and Purification of Recombinant BmSPN2 from E. coli. The average yield of His-BmSPN2 (with His-tag) was 7 mg/L culture, with a purity of >95% and an apparent molecular mass of ∼50 kDa on SDS−PAGE. Removal of the His-tag was accompanied by the expected 2 kDa reduction in size and loss of reactivity to Ni-NTA HRP conjugate. The identities of the pure proteins were confirmed by reactivity to antibody against recombinant BmSPN2 and by N-terminal sequencing (Supporting Information Figure I). CD spectra of His-BmSPN2, BmSPN2, and chicken ovalbumin (a noninhibitory serpin with a known structure) were similar in shape, indicating that they share a common fold (Supporting Information Figure II).

The two sequence variants of BmSPN2 (the original sequence (*9*) with Pro221 and Val225 and the new sequence with Ala221 and Ile225; Table 1) behaved identically in all experiments. Figure 2 shows the positions of these amino acid substitutions on the structure of antithrombin, the closest relative of BmSPN2 with a known structure. The presence of the His-tag on each protein had no effect on the results.

BmSPN2 Is Not an Inhibitor of Human Neutrophil Elastase and Cathepsin G. BmSPN2 did not inhibit the activities of

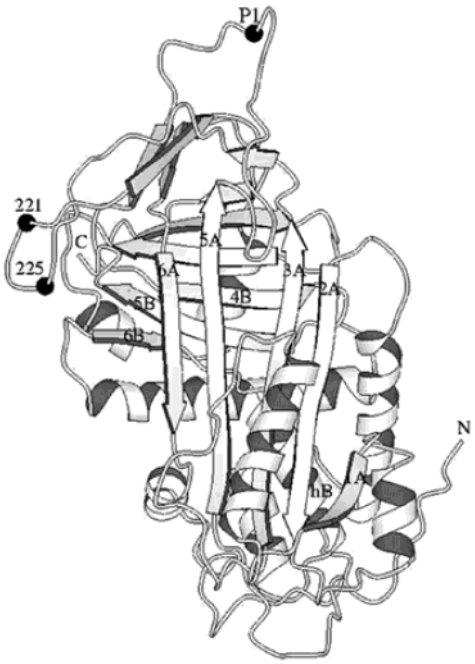

FIGURE 2: Serpin structure. Schematic picture (*33*) of the structure of human antithrombin III in its native form (*34*). Sequence alignment suggests that BmSPN2 shares the same fold. The N-terminus (N), C-terminus (C), the five strands of sheet A (1A, 2A, 3A, 5A, 6A), and the structural elements that make up the hydrophobic core of the molecule, helix B (hB) and strands four to six of sheet B (4B, 5B, 6B), are labeled. The sites of the sequence substitutions (221 and 225) are shown in the loop connecting strands three and four of sheet C.

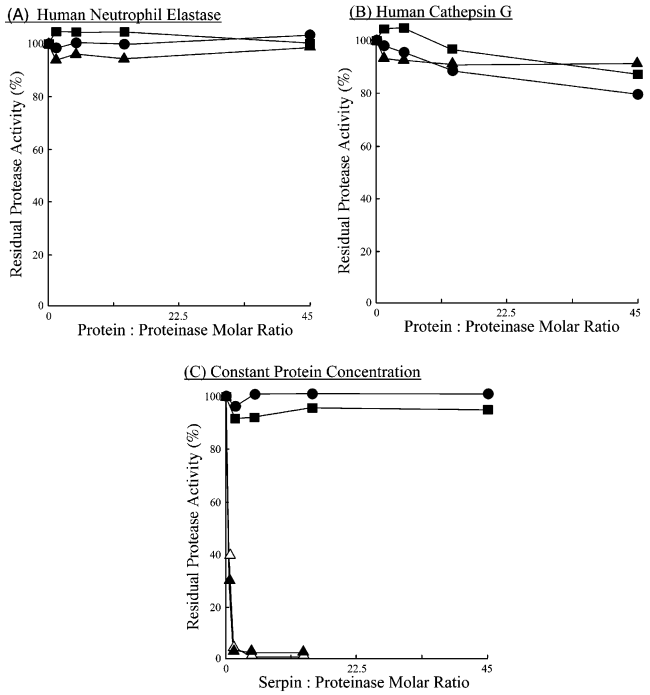

FIGURE 3: Failure of BmSPN2 to inhibit the activities of HNE and CatG. Concentration dependent proteinase inhibition assays at protein/proteinase molar ratios up to 45:1. BmSPN2 (circles) or BSA (squares) were incubated alone at 25 °C with either (A) HNE before the addition of 1.0 mM MeO-succinyl-Ala-Ala-Pro-Val-pNA or (B) CatG before the addition of 1.0 mM *N*-succinyl-Ala-Ala-Pro-Phe-pNA, as described. Changes in the rate of substrate cleavage were used to calculate the percentage of inhibition. Residual proteinase activities after incubation with BmSPN2 are also shown as a percentage of the activity after incubation with BSA (triangles). (C) Reactions between HNE (circles) or CatG (squares) with BmSPN2 as performed in panels A and B but with the addition of BSA to maintain the total protein concentration at 35 μM. Positive controls of antitrypsin with HNE (open triangles) and chymotrypsin with CatG (closed triangles) were performed under identical conditions.

HNE or CatG but at high concentrations did inhibit the ability of these enzymes to cleave a chromogenic substrate in solution. Figure 3A,B shows residual proteinase activities after incubation with BmSPN2 or BSA at protein/proteinase ratios up to 45:1. BmSPN2 or BSA had no effect on the rate of hydrolysis of the HNE substrate, *N*-methoxysuccinyl-Ala-Ala-Pro-Val-*p*-nitroanilide (assayed at 20 $\times$ K_M). However, high levels of BmSPN2 or BSA (reaching 35 μM) caused a reduction of up to 20% in the rate of hydrolysis of the CatG substrate, *N*-succinyl-Ala-Ala-Pro-Phe-*p*-nitroanilide (assayed at 0.5 $\times$ K_M). When the total amount of protein in the assay was kept constant with BSA, BmSPN2 showed no specific inhibition of either proteinase under the conditions examined (Figure 3C) (Supporting Information Figure III). The reactions of HNE with α1-antitrypsin and CatG with α1-antichymotrypsin were assayed under the same conditions as controls and showed inhibition as expected. Heparin, which enhances the activity of some inhibitory serpins, had no effect on BmSPN2.

No SDS-stable covalent complexes were detected when BmSPN2 was incubated with HNE or CatG (Figure 4), not even when serpin/proteinase molar ratios were increased to 20:1 and reactions performed at pH values ranging from 5 to 9.0 (Supporting Information Figures IV−VI). In contrast, HNE with α1-antitrypsin and CatG with α1-antichymotrypsin formed SDS-stable complexes under all conditions tested. Instead, BmSPN2 was found to be a very efficient substrate for both proteinases. In addition, BmSPN2 was shown to be a substrate for chymotrypsin, papain, subtilisin, trypsin, pancreatic elastase, V8 protease, Factor Xa, plasmin, thermolysin, thrombin, tPA, and urokinase.

Cleavage of the Reactive Center Loop. Incubation of BmSPN2 (50 kDa) with HNE at serpin/proteinase molar ratios between 50:1 and 10:1 gave a 43 kDa product (Figure 5A). Western blotting confirmed that the N-terminal His-tag was present only on this 43 kDa species and a 7 kDa band corresponding to the C-terminal leaving peptide was resolved on 16% polyacrylamide gels. Sequence analysis of the reaction mixture gave three sequences (Table 2). The major sequence was consistent with cleavage between residues 365 (P4) and 366 (P5) in the reactive center loop. Additional minor sequences corresponded to the N-terminus of intact BmSPN2 and a sequence starting 23 residues from the N-terminus. This latter sequence is consistent with secondary cleavage four amino acids C-terminal to the Factor Xa cleavage site, which would also remove the His-tag. Sites of cleavage were confirmed by resolving the proteolytic fragments with SDS−PAGE, transferring onto PVDF membrane, and sequencing individual bands. Following incubation of BmSPN2 with HNE at a serpin/proteinase molar ratio of 20:1, cleaved serpin was purified by capture on His-Bind resin. The C-terminal leaving peptide was detectable by SDS−PAGE in the eluted fraction showing that it remained attached to the larger N-terminal fragment unless liberated by denaturation.

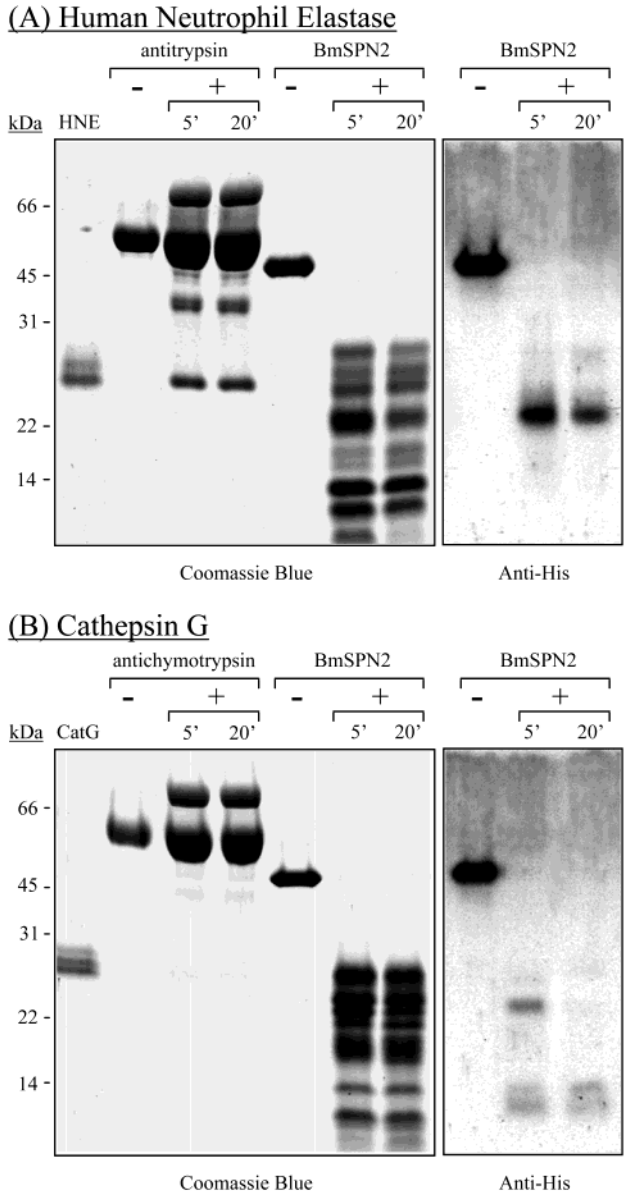

FIGURE 4: Failure of BmSPN2 to form a stable complex with HNE and CatG. Coomassie stained SDS−PAGE and anti-His HRP conjugate Western analysis of BmSPN2 reactions with (A) HNE and (B) CatG. BmSPN2 was incubated both without (−) and with (+) proteinase in reaction buffer at 25 °C for 5 and 20 min, and aliquots were electrophoresed on 10% SDS−PAGE under reducing conditions to detect the presence of inhibitory complexes. Positive controls of antitrypsin with HNE and antichymotrypsin with CatG were performed with their complexes appearing as higher MW bands. All lanes contained 7 μg of protein with a serpin/enzyme molar ratio of 4.5:1.

BmSPN2 Does Not Undergo the S to R Transition. The thermal stabilities of intact and HNE-cleaved BmSPN2 were compared with those of intact and *S. aureus* V8 proteinase-cleaved antitrypsin. Both serpins are cleaved at the P4−P5 bond. Native and cleaved BmSPN2 showed similar heat stabilities precipitating between 40 and 50 °C. Nondenaturing PAGE showed no evidence of polymers in heated samples. In contrast, native antitrypsin denatured between 50 and 60 °C, while the cleaved form remained stable to 80 °C, as previously described (*4*, *16*) (Supporting Information Figure VII).

CD spectroscopy showed minimal change in the overall conformation of BmSPN2 after loop cleavage (Figure 5A).

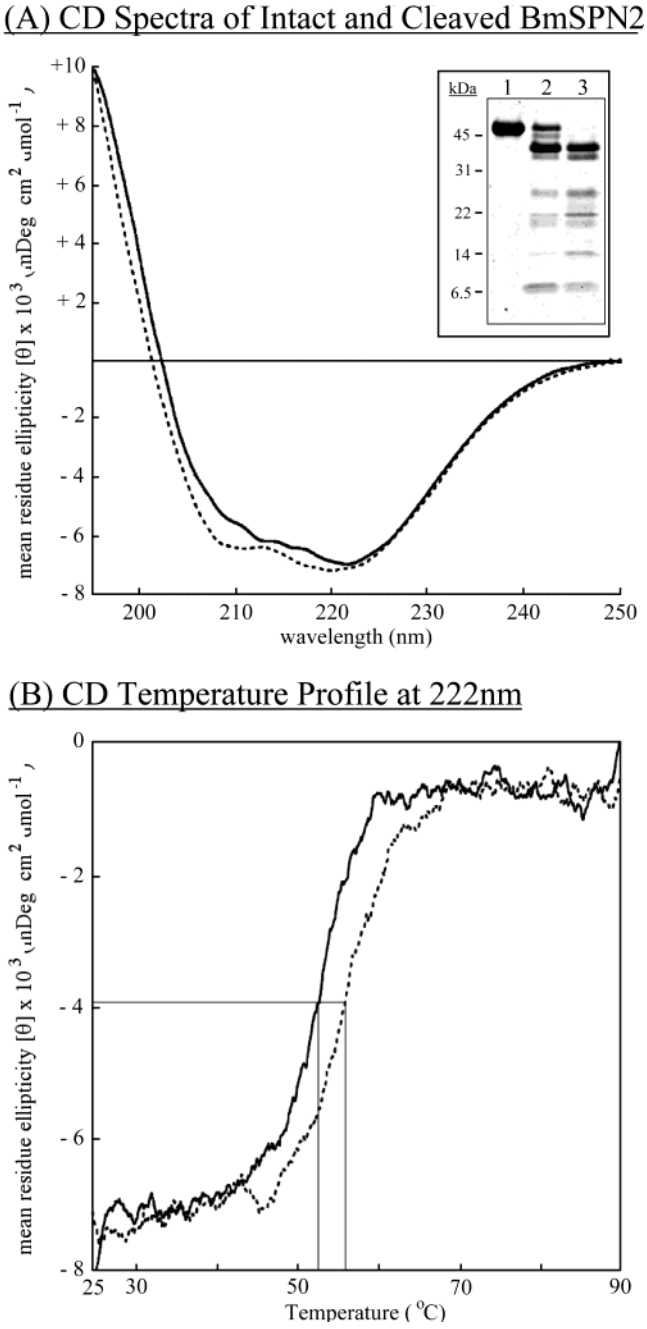

FIGURE 5: Thermal stability of BmSPN2 determined by circular dichroism. (A) Far-ultraviolet CD spectra of intact (solid line) and HNE cleaved (dashed line) BmSPN2. The spectra shown are averages of at least two separately run spectra. Spectra were recorded at 25 °C in 10 mM phosphate buffer, pH 7.9 with a protein concentration of 0.15 mg/mL. Inset, a Coomassie stained 12.5% SDS−PAGE gel run under reducing conditions showing BmSPN2 alone (lane 1) and incubated with HNE at molar ratios of 50:1 (lane 2) and 25:1 (lane 3) for 20 min at 25 °C. (B) CD signal at 222 nm for intact (solid line) and HNE cleaved (dashed line) BmSPN2 while increasing the sample temperature at 1 °C/min. The unit on the ordinate is mean residue ellipticity.

Changes in CD ellipticity at 222 nm followed similar unfolding profiles for native and cleaved forms of BmSPN2 with only a slight increase in stability (T_m 52.4 vs 56.0 °C) on cleavage (Figure 5B).

The urea-induced unfolding transitions of native and cleaved BmSPN2 were compared with those of an antitrypsin control (Figure 6). Native and cleaved BmSPN2 behaved identically, unfolding proportionately with increasing urea

Table 2: Summary of Sequence Analysis of His-BmSPN2 Proteolytic Fragments

size of peptide (kDa)[a]	N-terminal sequence[b]	yield (pmol)
50.0	GHHHHHHH	4
47.3	(23) TLNHCSEN	2
42.7	GHHHHHHH	4
40.0	(23) TLNHCSEN	2
7.4	(366) RNDMVMDK	30

[a] Estimated from SDS−PAGE [b] Amino acids are given in single letter code. Numbering corresponds to the derived sequence from the *Bm-spn-2* cDNA where residue 1 is the first position for the precursor BmSPN2 polypeptide and position 21 corresponds to the first residue of the mature protein (*9*).

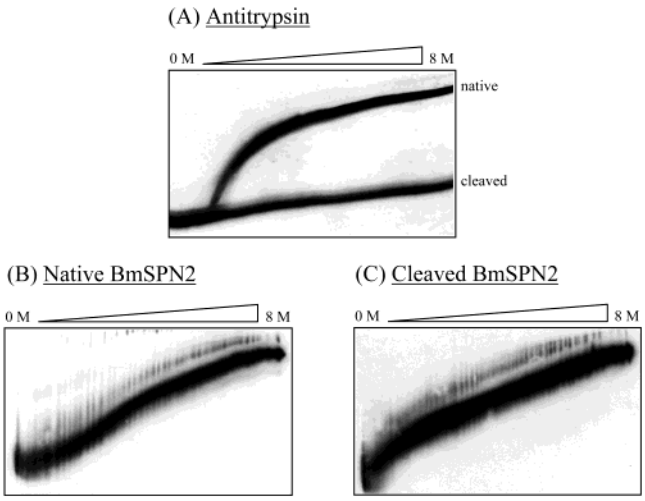

FIGURE 6: Transverse urea gradient gel electrophoresis of BmSPN2. The urea-induced unfolding transitions of (A) 50 μg of native mixed with 50 μg of *S. aureus* V8-cleaved human antitrypsin, Coomassie stained; (B) 5 μg of uncleaved BmSPN2 and (C) 5 μg of HNE-cleaved BmSPN2 reacted with anti-His HRP conjugate on a 10% (w/v) polyacrylamide nondenaturing gel. The left of each gel represents 0 M urea and the right 8 M urea.

concentration. In contrast, native antitrypsin showed decreased mobility as it unfolded at approximately 1.5 M urea, while cleaved antitrypsin failed to unfold even in 8 M urea (*11*, *15*).

Sequence and Structural Comparison with Other Serpins. A search for sequences homologous to BmSPN2 using Psi-BLAST resulted in 503 blast hits with other serpins. The highest sequence identity was 28% with BmSPNl, but most other serpins showed sequence identities in the 18−24% range. Sequence alignment of BmSPN2 with the most closely related serpins that have a known structure (antithrombin III, ovalbumin, plasminogen activator inhibitor-2, and leukocyte elastase inhibitor) suggested that BmSPN2 shares the tertiary structure typical of the family as a whole (Figure 2). The buried apolar segments of the structure (helix B, strands 4B, 5B, and 6B) are the most highly conserved regions, but all other secondary structure elements appear to be present in BmSPN2. BmSPN2 has a C-terminal extension of some 20 residues as compared to typical serpins. The reactive site sequence shows features consistent with a noninhibitory serpin, as discussed below (Figure 1). The residues that differ in the two variants of BmSPN2 (221 and 225) are both found within a loop connecting strands three and four of β-sheet C.

DISCUSSION

Previous work by Zang et al. (*9*) described the expression of BmSPN2 in *E. coli*, and the finding that the protein could inhibit the activities of HNE and CatG. We have re-isolated the *Bm-spn-2* gene from a separate microfilarial cDNA library, expressed the gene product in *E. coli*, and carried out a detailed examination of the structural and functional characteristics of purified BmSPN2. The protein expressed by Zang et al. contained a nonsense N-terminal extension and a noncleavable C-terminal $(His)_6$-tag. We have expressed mature BmSPN2 with a cleavable N-terminal His-tag and have shown that its presence has no effect. The sequence of the protein we isolated had two amino acid substitutions (P221A and V225I) as compared to Zang et al.'s protein (*9*). It is likely that both proteins represent natural variants as both sequences were verified from independent clones after PCR. The presumed sites of these substitutions are in a part of the serpin structure unaltered during the S to R conformational change that accompanies proteinase inhibition and reactive loop cleavage (Figure 2), suggesting that they would not influence inhibitory activity. We have expressed and purified both variants in this work and found that they behaved identically in all our experiments.

The sequence of the reactive center loop in BmSPN2 contrasts dramatically with the consensus loop sequence for inhibitory serpins. It is well-established that the proximal hinge (P15-P10) of the reactive center loop of inhibitory serpins contains residues with small aliphatic side chains (*17*, *18*) providing the flexibility that is needed for the cleaved loop to insert into β-sheet A during proteinase inhibition. In most noninhibitory serpins there is no functional requirement for loop insertion, and proximal hinge residues have bulky or charged side chains that would interfere with this transition (Figure 1). The hinge sequence in BmSPN2 from P15-P10 (GINNEN) together with a proline at P6 would be expected to block insertion of the N-terminal end of the loop into sheet A and is incompatible with the adoption of a β-conformation. Furthermore, it is likely that the conformational change involved in opening β-sheet A would fail to take place. Residues involved in packing at the interfaces where movement takes place are strongly conserved in serpins that undergo the conformational change (*19*) but show critical changes in BmSPN2 (including a tryptophan at position 397 replacing a conserved phenylalanine and changes in helix F). This strongly suggests that BmSPN2 could not inhibit proteinases by the standard serpin mechanism. Despite this, BmSPN2 has been reported as being an inhibitor of neutrophil elastase and cathepsin G (*9*). Here, we resolve this apparent paradox and show definitively that BmSPN2 does not inhibit the activities of HNE and CatG (Figure 3) and does not form complexes with these enzymes (Figure 4) or with a range of other serine proteinases. Our results show that BmSPN2 is in fact a good substrate for both HNE and CatG. Limited proteolysis of BmSPN2 with HNE results in cleavage between P4 and P5, suggesting that BmSPN2 has a proteinase-sensitive exposed loop in common with most other serpins. The vulnerability of the reactive center loop to proteolysis confirms that it is already in an exposed and accessible conformation. Therefore, lack of inhibitory activity in BmSPN2 cannot be explained either by the protein having adopted a latent conformation (in which the intact reactive

center loop is inserted in sheet A of the same molecule) or a requirement for cofactor activation to expel the loop from a folded position in sheet A.

The stability of BmSPN2 to denaturation by heat (Figure 5) or urea (Figure 6) does not increase significantly on loop cleavage. Cleaved BmSPN2 is only slightly more stable to heat (T_m 4 °C higher) than the native form, in marked contrast to the large increase on cleavage of inhibitory serpins (T_m more than 40 °C higher) (*20*, *21*). This suggests that loop cleavage of BmSPN2 is not associated with the conformational change from stressed (S) to relaxed (R) forms as is typically observed for inhibitory serpins. The thermal stability curves of BmSPN2 resemble those of two noninhibitory serpins, angiotensinogen (*5*) and pigment epithelium-derived factor (*22*). Ovalbumin appears to be thermodynamically more stable, denaturing at temperatures about 20 °C higher (*23*).

We have shown that BmSPN2 is structurally incapable of irreversible proteinase inhibition typical of a serpin. The earlier suggestion (*9*) that BmSPN2 showed inhibitory activity is probably explained by reversible inhibition through competition between BmSPN2 acting as an enzyme substrate and the chromogenic substrate (Supporting Information Figure VIII). This effect was made more obvious by the use of exceptionally large amounts of proteinase (7 μM) and serpin (up to 80 μM or 4 mg/mL) and the use of enzyme substrates with exceptionally high K_M values, particularly that for HNE, which is more commonly used as a substrate for pancreatic elastase. Reversible inhibition of HNE or CatG by a thermally induced conformer of ovalbumin (I-Ov) has been described (*24*). In contrast to BmSPN2, however, I-Ov has a structure different to that of native ovalbumin as judged by CD spectroscopy, it remains uncleaved by the enzymes, and it is a highly specific inhibitor acting at nanomolar concentrations. In fact, the inhibition by BmSPN2 is similar to that produced by serum albumin in assays performed under conditions previously reported (*9*) and can have no biological significance (Supporting Information Figure XI).

Since BmSPN2 is expressed exclusively by *B. malayi* microfilariae and is secreted into the blood, a likely role for this serpin is in helping the parasite to evade the human immune response. It was proposed that BmSPN2 achieved this aim by inhibiting the activities of human neutrophil proteinases (*9*), but we show that this cannot be true. Another possibility is that BmSPN2 may act as a costimulus for IgG4 switching associated with a shift in the cytokine balance from a Th1 to a Th2 response (*25*). A similar role has been reported for the serpin antitrypsin where, intriguingly, its effect is at least partially independent of its proteinase inhibitory activity (*26*).

We have provided evidence that BmSPN2 has a tertiary structure resembling typical members of the serpin family with an exposed reactive center loop. However, BmSPN2 shows no proteinase inhibitory activity and cannot undergo the S to R transition that forms an integral part of the serpin inhibitory mechanism. This work corrects the previous assertion that BmSPN2 inhibits neutrophil elastase and cathepsin G. The physiological target of BmSPN2 remains unknown, but a role as a stage-specific protein in promoting parasite survival and protection from the human immune response is most likely.

ACKNOWLEDGMENT

We are grateful to Prof. Rick Maizels, Prof. Robin Carrell, and Dr. Didier Belorgey for helpful discussions in the preparation of this manuscript.

SUPPORTING INFORMATION AVAILABLE

Gels for BmSPN2 purification, absence of SDS-stable complexes, and thermal stability; CD spectra for BmSPN2 and ovalbumin; and additional proteinase activity assays. This material is available free of charge via the Internet at http://pubs.acs.org.

REFERENCES

1. Travis, J., and Salvesen, G. S. (1983) *Annu. Rev. Biochem. 52*, 655−709.
2. Silverman, G. A., Bird, P. I., Carrell, R. W., Church, F. C., Coughlin, P. B., Gettins, P. G., Irving, J. A., Lomas, D. A., Luke, C. J., Moyer, R. W., Pemberton, P. A., Remold-O'Donnell, E., Salvesen, G. S., Travis, J., and Whisstock, J. C. (2001) *J. Biol. Chem. 276*, 33293−33296.
3. Huntington, J. A., Read, R. J., and Carrell, R. W. (2000) *Nature 407*, 923−926.
4. Carrell, R. W., and Owen, M. C. (1985) *Nature 317*, 730−732.
5. Stein, P. E., Tewkesbury, D. A., and Carrell, R. W. (1989) *Biochem. J. 262*, 103−107.
6. Dafforn, T. R., Della, M., and Miller, A. D. (2001) *J. Biol. Chem. 276*, 49310−49319.
7. Pemberton, P. A., Stein, P. E., Pepys, M. B., Potter, J. M., and Carrell, R. W. (1988) *Nature 336*, 257−258.
8. Yenbutr, P., and Scott, A. L. (1995) *Infect. Immun. 63*, 1745−1753.
9. Zang, X., Yazdanbakhsh, M., Jiang, H., Kanost, M. R., and Maizels, R. M. (1999) *Blood 94*, 1418−1428.
10. Williams, S. A., and Johnston, D. A. (1999) *Parasitology 118*, S19−38.
11. Lomas, D. A., Elliott, P. R., Chang, W. S., Wardell, M. R., and Carrell, R. W. (1995) *J. Biol. Chem. 270*, 5282−5288.
12. Lawrence, D. A., Olson, S. T., Palaniappan, S., and Ginsburg, D. (1994) *J. Biol. Chem. 269*, 27657−27662.
13. Schagger, H., and von Jagow, G.(1987) *Anal. Biochem. 166*, 368−379.
14. Lomas, D. A., Finch, J. T., Seyama, K., Nukiwa, T., and Carrell, R. W. (1993) *J. Biol. Chem. 268*, 15333−15335.
15. Mast, A. E., Enghild, J. J., Pizzo, S. V., and Salvesen, G. (1991) *Biochemistry 30*, 1723−1730.
16. Lomas, D. A, Evans, D. L., Stone, S. R., Chang, W. S., and Carrell, R. W. (1993) *Biochemistry 32*, 500−508.
17. Hopkins, P. C., Carrell, R. W., and Stone, S. R. (1993) *Biochemistry 32*, 7650−7657.
18. Patston, P. A., and Gettins, P. G. (1996) *FEBS Lett. 383*, 87−92.
19. Stein, P., and Chothia, C. (1991) *J. Mol. Biol. 221*, 615−621.
20. Gettins, P., and Harten, B. (1988) *Biochemistry 27*, 3634−3639.
21. Hood, D. B., Huntington, J. A., and Gettins, P. G. (1994) *Biochemistry 33*, 8538−8547.
22. Becerra, S. P., Sagasti, A., Spinella, P., and Notario, V. (1995) *J. Biol. Chem. 270*, 25992−25999.
23. Smith, M. B., and Back, J. F. (1968) *Aust. J. Biol. Sci. 21*, 539−548.
24. Mellet, P., Michels, B., and Bieth, J. G. (1996) *J. Biol. Chem. 271*, 30311−30314.
25. Zang, X., Atmadja, A. K., Gray, P., Allen, J. E., Gray, C. A., Lawrence, R. A., Yazdanbakhsh, M., and Maizels, R. M. (2000) *J. Immunol. 165*, 5161−5169.
26. Jeannin, P., Lecoanet-Henchoz, S., Delneste, Y., Gauchat, J. F., and Bonnefoy, J. Y. (1998) *Eur. J. Immunol. 28*, 1815−1822.
27. Bollen, A., Herzog, A., Cravador, A., Herion, P., Chuchana, P., van der Straten, A., Loriau, R., Jacobs, P., and van Elsen, A. (1983) *DNA 2*, 255−264.
28. Chandra, T., Stackhouse, R., Kidd, V. J., Robson, K. J., and Woo, S. L. (1983) *Biochemistry 22*, 5055−5061.
29. Bock, S. C., Wion, K. L., Vehar, G. A., and Lawn, R. M. (1982) *Nucleic Acids Res. 10*, 8113−8125.
30. Gaillard, I., Clauser, E., and Corvol, P. (1989) *DNA 8*, 87−99.

31. Woo, S. L., Beattie, W. G., Catterall, J. F., Dugaiczyk, A., Staden, R., Brownlee, G. G., and O'Malley, B. W. (1981) *Biochemistry 20*, 6437−6446.
32. Steele, F. R., Chader, G. J., Johnson, L. V., and Tombran-Tink, J. (1993) *Proc. Natl. Acad. Sci. U.S.A. 90*, 1526−1530.
33. Kraulis P. (1991) *J. Appl. Crystallog. 24*, 946−950.
34. Carrell, R. W., Stein, P. E., Fermi, G., and Wardell, M. R. (1994) *Structure 2*, 257−270.

BI0271650